

Classification of First-Episode Schizophrenia, Chronic Schizophrenia and Healthy Control Based on Brain Network of Mismatch Negativity by Graph Neural Network

Qi Chang, Cancheng Li[✉], Graduate Student Member, IEEE, Qing Tian[✉], Qijing Bo[✉], Jicong Zhang[✉], Yanbing Xiong, and Chuanyue Wang[✉]

Abstract— Mismatch negativity (MMN) has been consistently found deficit in schizophrenia, which was considered as a promising biomarker for assessing the impairments in pre-attentive auditory processing. However, the functional connectivity between brain regions based on MMN is not clear. This study provides an in-depth investigation in brain functional connectivity during MMN process among patients with first-episode schizophrenia (FESZ), chronic schizophrenia (CSZ) and healthy control (HC). Electroencephalography (EEG) data of 128 channels is recorded during frequency and duration MMN in 40 FESZ, 40 CSZ patients and 40 matched HC subjects. We reconstruct the cortical endogenous electrical activity from EEG recordings using exact low-resolution electromagnetic tomography and build functional brain networks based on source-level EEG data. Then, graph-theoretic features are extracted from the brain networks with the support vector machine (SVM) to classify FESZ, CSZ and HC groups, since the SVM has good generalization ability and robustness as a universally applicable nonlinear classifier. Furthermore, we introduce

Manuscript received December 23, 2020; revised May 4, 2021 and June 29, 2021; accepted July 14, 2021. Date of publication August 18, 2021; date of current version September 10, 2021. This work was supported in part by Beijing Natural Science Foundation under Grant Z200024, in part by the National Key Research and Development Program of China under Grant 2016YFF0201002, and in part by the University Synergy Innovation Program of Anhui Province under Grant GXXT-2019-044. (Corresponding authors: Jicong Zhang; Yanbing Xiong; Chuanyue Wang.)

This work involved human subjects or animals in its research. Approval of all ethical and experimental procedures and protocols was granted by Beijing Anding Hospital Ethics Committee.

Qi Chang and Cancheng Li are with the School of Biological Science and Medical Engineering, Beihang University, Beijing 100083, China, and also with Beijing Advanced Innovation Centre for Biomedical Engineering, Beihang University, Beijing 100083, China.

Qing Tian, Qijing Bo, and Chuanyue Wang are with Beijing Anding Hospital, Capital Medical University, Beijing 100088, China (e-mail: wang.cy@163.net).

Jicong Zhang is with the School of Biological Science and Medical Engineering, Beihang University, Beijing 100083, China, also with Beijing Advanced Innovation Centre for Biomedical Engineering, Beihang University, Beijing 100083, China, and also with Hefei Innovation Research Institute, Beihang University, Hefei 230012, China (e-mail: jicongzhang@buaa.edu.cn).

Yanbing Xiong is with the Psychiatry Department, Shanxi Bethune Hospital, Shanxi Academy of Medical Sciences, Tongji Shanxi Hospital, Third Hospital of Shanxi Medical University, Taiyuan 030032, China (e-mail: bearybing@163.com).

This article has supplementary downloadable material available at <https://doi.org/10.1109/TNSRE.2021.3105669>, provided by the authors.

Digital Object Identifier 10.1109/TNSRE.2021.3105669

the graph neural network (GNN) model to directly learn for the network topology of brain network. Compared to HC, the damaged brain areas of CSZ are more extensive than FESZ, and the damaged area involved the auditory cortex. These results demonstrate the heterogeneity of the impacts of schizophrenia for different disease courses and the association between MMN and the auditory cortex. More importantly, the GNN classification results are significantly better than those of SVM, and hence the EEG-based GNN model of brain networks provides an effective method for discriminating among FESZ, CSZ and HC groups.

Index Terms— Classification, functional brain connectivity, graph neural network, mismatch negativity, schizophrenia.

I. INTRODUCTION

COGNITIVE impairment is considered to be a core symptom of schizophrenia, that should be taken into consideration along with other negative and positive core symptoms [1]. Cognitive functions include advanced information processing functions as well as elementary sensory functions, including auditory functions. Mismatch negativity (MMN) is an event-related potential (ERP) that reflects the pre-attentive auditory processing capability [2]. One key conclusion of the initiative for Cognitive Neuroscience Treatment Research to Improve Cognition in Schizophrenia (CNTRICS) is that MMN, as an electrophysiological indicator, is one of the most promising schizophrenia biomarkers [3]. Moreover, previous studies have found MMN deficits in patients with first-episode schizophrenia (FESZ) [4], [5], chronic schizophrenia (CSZ) [6], [7] and ultra-high-risk (also known as clinical-risk) subjects [8], [9].

Auditory MMN is induced by the oddball paradigm, which consists of a series of repeated identical standard stimuli with a few randomly dispersed deviant stimuli [10]. The deviant stimuli differ from the standard ones in physical characteristics, particularly in frequency and duration. While both stimulus types have been extensively studied, there is no clear consensus on the differences between the two types in patients with FESZ and CSZ, and healthy control (HC). In a recent study [11], a literature survey was conducted on whether duration MMN and frequency MMN were significantly reduced in the first-episode schizophrenic patients compared to healthy subjects. The review has shown that

most studies have demonstrated a significant reduction of the duration MMN in FESZ patients, but no studies found reduction in the frequency MMN. Moreover, a previous study [12] showed larger changes in the duration MMN than in the frequency MMN. The afore-mentioned findings may indicate that the duration MMN is more sensitive than the frequency MMN in differentiating between schizophrenic and healthy subjects. Therefore, understanding the neural mechanism of MMN damage in different schizophrenic stages is helpful to understand the disease progression process of schizophrenic patients, and it can also help to understand the differences of different deviations.

The MMN signals are essentially generated in brain regions within the bilateral supratemporal cortex [13]–[15] and the frontal lobe [14], [16]–[18]. In recent years, there is a mature hypothesis about the mechanism of MMN generation called predictive coding [19], [20]. The hypothesis of predictive coding suggests that the inferior frontal gyrus (IFG) processes the next auditory signal according to the auditory memory template formed by repeated standard stimuli in the superior temporal gyrus (STG), and STG will send out the prediction error signal to IFG when deviant stimuli are introduced. schizophrenic patients exhibited disorders of functional interactions between brain regions [21], as well as cognitive impairments [22]. There are numerous research papers on schizophrenia resting-state functional connectivity. A recent review [23] summarized the significantly different connections in the FESZ and CSZ groups compared to the HC based on resting state functional MRI, and concluded that 90% affected regions in FESZ involves frontal lobes, while differences in CSZ are more extensive. In a study [24] that reviewed functional and structural neuroimaging studies using task or resting-state in ultra-high risk, FESZ, and CSZ stages of schizophrenia, it was shown that schizophrenia is associated with connectivity reductions compared with HC, which is particularly evident in the frontal lobe and applies to all stages of schizophrenia.

The functional brain network based on resting state functional magnetic resonance imaging (fMRI) found that the connectivities involved auditory cortex of schizophrenia patients were abnormal, and the additional model using MMN variables as covariates showed that the abnormal connectivities of frequency MMN are mainly limited to the auditory cortex, while the connection abnormality of duration MMN is more diffuse [25]. Dima *et al.* [26] used dynamic causal models based on magnetoencephalography (MEG) data of frequency MMN and studied abnormal intrinsic and extrinsic connectivities in the primary auditory area (A1), STG and IFG in schizophrenia. The results suggest that the local neuronal adaptation of the auditory cortex has been impaired in patients with schizophrenia, and its connection to the higher-order cortex has been also damaged. Koshiyama *et al.* [27] analyzes abnormal effective connectivity based on MMN in schizophrenia, and the results showed that the dynamic interaction between temporal and frontal sources is the basis of MMN abnormality in schizophrenia. However, differences in brain region connectivities between the FESZ, CSZ and HC groups have not been addressed. Furthermore, it was found that

different types of deviant stimuli can activate specific brain regions that are few millimeters apart [13], [28]. However, the brain region connectivity patterns for different deviant stimuli in the FESZ, CSZ and HC groups are not clear.

A high-performance computer-aided schizophrenia diagnosis system can be useful as a clinical decision-support tool. The diagnosis of schizophrenia is of great significance, and diagnosis based on electroencephalogram (EEG) is particularly convenient and of low-cost. EEG as an auxiliary diagnostic method for schizophrenia, preliminary approaches for schizophrenia diagnosis exploited resting-state EEG signals. Besides, schizophrenia diagnosis has also been achieved using task-related EEG signals analysis methods such as P300 [29], [30], press button task [31], [32], and the working memory analysis [33]. To be specific, many researchers explored different features for schizophrenia diagnosis using EEG signals like the time-domain features, frequency-domain features, and combinations of these features [34]–[36]. Many classifiers have been exploited for schizophrenia diagnosis including support vector machines (SVM) [29], [30], linear discriminant analysis (LDA) [37], [38], and convolutional neural networks (CNN) [39], [40].

Most of the existing methods for schizophrenia diagnosis employ sensor-level EEG signals [35], [39]. The corresponding source-space signals are obtained through inversion of the sensor-level EEG signals along with the exploitation of the anatomical prior information, which reflects the local neural activities in the cortex with a satisfactory spatial resolution. Source-space features could then be extracted to improve the classification accuracy [30]. In addition, the realization of the brain functions depends on the information communication and integration among the brain regions. This motivates the investigation of brain disorders based on functional brain networks (or graphs). However, neural-network classifiers (such as the CNN ones) cannot be directly applied to graph data, which is defined by nodes and edges. Recently, GNN has been proposed as an adaptation of classical deep learning models for graph data [41], [42]. This type of neural networks successfully models the rich dependencies among nodes in a graph. Various GNN applications have been developed to solve the problems of natural and social sciences [43]–[45]. These applications demonstrate convincing performance and high interpretability of GNNs. Therefore, we introduce a graph neural network (GNN) model to effectively learn the topological structure of source-space brain networks in order to boost the state-of-the-art performance in early schizophrenia diagnosis.

In summary, in order to address the issues in brain functional connectivity based on MMN and in existing methods to identify schizophrenia, the main contributions of this paper are as follow. First of all, we construct source-level brain connectivity based on dense-array EEG data of both frequency and duration deviant stimuli MMN and identify the differences in brain connectivity between the FESZ, CSZ and HC groups. This provides evidences for exploring the neural mechanism of MMN damage in different stages of schizophrenia and reveals the connectivity patterns of different deviant stimuli in the FESZ, CSZ and HC groups. Furthermore, we develop a novel framework for early recognition of schizophrenia,

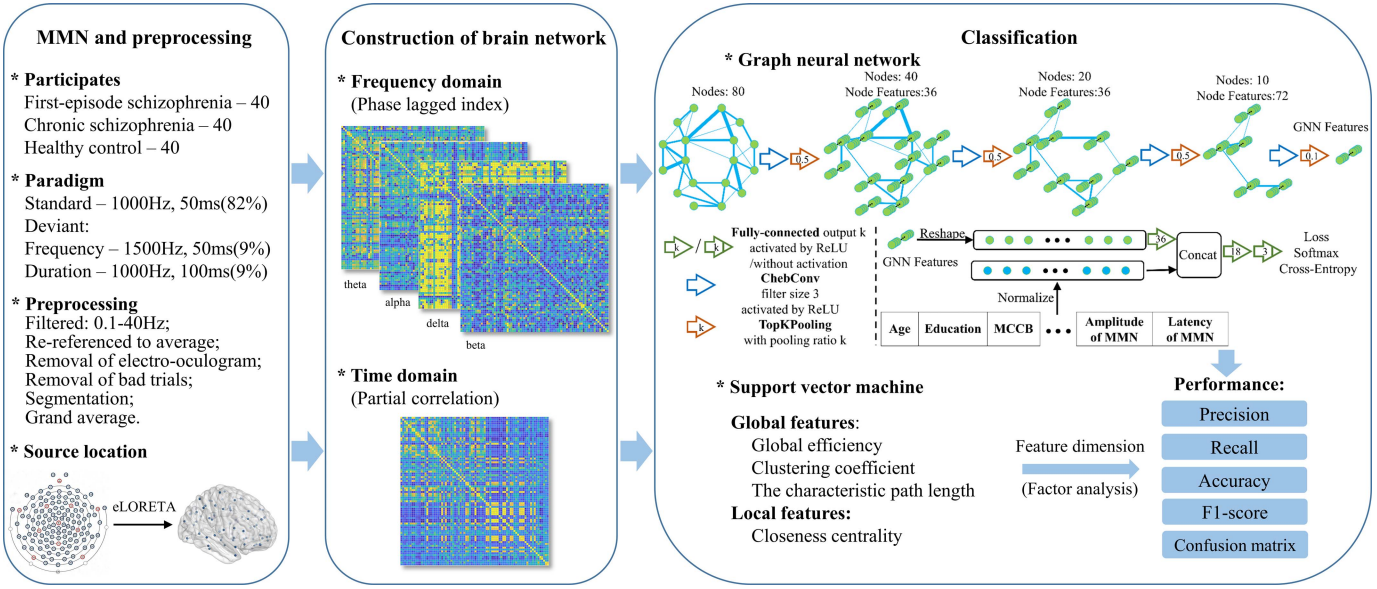


Fig. 1. Flow chart of this study. The work flow of the system is three parts. Firstly, MMN recording of two kinds of deviant stimuli is collected from first-episode schizophrenia patients, chronic schizophrenia patients, and healthy control. Secondly, two approaches are used to construct brain network from frequency domain and time domain. Thirdly, a graph neural network (GNN) is constructed for diagnosis, which takes both brain network and the demographic information as input, and generate the potential category of a patient.

specifically, GNN is introduced to learn the network topology of brain networks in the source space, which could better obtain the complex relationships in the MMN disorder mechanism of schizophrenia. Moreover, the cognitive features of the MATRICS Consensus Cognitive Battery (MCCB) and sensor-level features of amplitude and latency of MMN are introduced to be combined with the electrophysiological features to assist classification. Besides, we also utilize the SVM to learn global and local features based on graph theory for the brain networks and compare it with GNN classifier in performance. It is worth mentioning that we detect FESZ from CSZ and HC in this paper, which could help effectively identify schizophrenia in the early stage. The flow chart of our study is shown in Fig. 1.

II. MATERIALS AND METHODS

A. Participants and EEG Recording

The dataset used in this study consist of 40 FESZ, 40 CSZ and 40 age-, gender- and education- matched HC subjects. An auditory oddball paradigm based on frequency and duration deviant stimuli on the subjects has been performed. The details of the dataset and paradigm are available in *Supplementary Materials* and in [46].

The EEG data was recorded by a 128-channel monitoring device manufactured by Electrical Geodesics, Inc. with the Cz site as the reference. The impedance of each electrode was controlled to be below $5\text{k}\Omega$ and the sampling rate was 1000 Hz. The collected data was bandpass filtered from 0.1 to 100 Hz. Subjects were seated in comfortable backrest seats in an electromagnetically-shielded room with appropriate lights and no noise. For the auditory experiments, participants were asked to stare at a black cross in the center of the screen, which was about 50 cm in front of them.

B. Preprocessing

Preprocessing of the EEG data was performed in MATLAB. The data was filtered by a bandpass filter with a pass band of 0.1–40 Hz, and then the filtered data was re-referenced to its average value. Electrooculogram (EOG) artifacts were removed through the independent component analysis (ICA) algorithm. Bad electrodes were also detected and removed. Each event-related potential (ERP) trial was inspected manually and the ones which contained artifacts were also removed.

Each ERP segment was extracted starting from 100 ms before the onset of the stimulus to 500 ms after the stimulus presentation where the first 100-ms interval was used as a baseline correction. After averaging the trials with the two kinds of deviant stimuli, the standard-stimulus trial waveforms were subtracted to obtain two types of MMN waveforms. For each segment, the MMN component was identified as the maximum negative peak between 100 ms and 250 ms after the stimulus onset, which was used for subsequent analysis.

C. Construction of Brain Networks

The EEG is a microvolt-level superimposed electrical signal that is generated by many neurons in the cortex and discharged to the scalp through the uneven impedance of the skull. The accuracy of EEG measurement and superposition is not conducive to our analysis of the activity within the cortex. Therefore, the exact low-resolution electromagnetic tomography (eLORETA) intra-brain signal source-imaging method was used to first restore and map the intracortical EEG source signals, which were then used to construct and analyze the brain networks [47], [48]. The above preprocessing may lead to interference from non-MMN signals. To prevent this undesirable interference, we used the segments between 100–250 ms after the stimulus onset to reconstruct the cortical endogenous time series using eLORETA. The central voxels

of the 80 AAL-based brain regions [47], [49] were selected as nodes of the functional network where each hemisphere has 40 regions, and the coordinates of each node are included in the appendix. Two approaches for constructing a brain network were followed. One approach is based on the partial correlation (PC) coefficient, which measures the linear correlation between each two nodes using the amplitude and phase information. The other approach is based on the phase lag index (PLI), which is a measure of the asymmetry of the distribution of the phase difference between signal pairs. Compared to other phase synchronization measures, this measure is much less affected by volume conduction and active reference electrodes. When applying PLI, we filtered MMN into four frequency bands, namely delta (1.5–4 Hz), theta (4–8 Hz), alpha (8–13 Hz) and beta (13–30 Hz). Further details of partial correlation and phase lag index are given in *Supplementary Materials*.

Besides, brain networks of the three groups (FESZ, CSZ and HC) were compared, and connectivities with significant differences were extracted by the permutation test ($p < 0.01$).

D. Classification

1) The Support Vector Machine (SVM) Classifier: The aforementioned features were used to train and test a SVM classifier to differentiate between the FESZ, CSZ and HC subjects. The SVM classifier can be equipped with kernel functions of different types. In this paper, we employed a SVM with a radial basis function (RBF) [50] since this kernel function can map the input features to a higher-dimensional space with fewer parameters and better performance for both large and small numbers of samples. The exploited features (or characteristics) can be divided into four groups: demographic characteristics, MCCB, ERP performance, and brain network characteristics. Firstly, the demographic characteristics are three in total, namely age, years of education, and intelligence quotient (IQ). Secondly, the MCCB has 8 characteristics, including seven assessment scores and one overall composite score. Thirdly, the ERP performance characteristics are 4, namely the amplitude and latency of MMN. Finally, the brain network characteristics can be computed for the construction based on the partial correlation coefficient or that based on the PLI. In particular, local and global network parameters were computed to measure the characteristics of the built networks. Among them, global parameters include global efficiency, global clustering coefficient and the characteristic path length. As for the characteristics of the node as local parameters, considering that many nodes have a value of zero in betweenness centrality [51] and it not conducive to learning and classification, closeness centrality [52] was selected to characterize the stability of the node in the network. The calculation formula of the brain network parameters was shown in the *Supplementary Materials*.

Thus, for each of these two constructions, we calculated the same set of features: the characteristic path length (1), the global efficiency (1), the global clustering coefficient (1) and the closeness centrality for each node (80). This gives a total of 83 features. Considering that too many features will lead to overfitting of the classification model, we used

factor analysis to reduce the dimensions of 83 brain network features in each training, retaining the factors with eigenvalue above 1 [53]. SPSS 22 software was used for factor analysis.

Therefore, there are 10 conditions for classification: four frequency bands (alpha, beta, theta and delta) during the PLI-based network construction and one partial-correlation-based network without frequency-band filtering in frequency MMN and the duration MMN, respectively. For each condition, there are 3 demographic characteristics, 8 MCCB parameters, 2 ERP and 3~21 brain network features (the number of brain network features in each condition was shown in Table A.1 of *Supplementary Materials*).

2) The Graph Convolutional Neural Network (GCNN) Classifier: Convolutional neural networks (CNNs) have a lot of remarkable applications and significant breakthroughs in video, image and sound recognition problems [54]. The success of CNNs could be attributed to their hierarchical structures, which enable them to extract and integrate multi-scale features from data in the Euclidean domain. Data in non-Euclidean domains (e.g. social networks, gene data, and brain networks) could be encoded by graphs, which not only include quantified elements, but also the relationships among them.

The GCNNs can effectively combine data-driven approaches with graphical models. Apart from traditional graphical models (such as the Markov random field model), GCNNs could create sophisticated feature representations for high-level automated reasoning. Moreover, GCNNs demonstrate higher scalability to big data and better capacity for inference based on multiple graphs.

In this paper, a graph is denoted as $G = (V, E, A)$, where V and E are, respectively, two sets of vertices and associated edges, while A denotes a weighted adjacency matrix. Let the number of vertices be n , i.e., $|V| = n$. The dataset of schizophrenic and healthy subjects is denoted as $D = \{(G_n, I_n, y_n) | n = 1, 2, 3 \dots N\}$, where N is the number of graphs (or observations), G_n denotes the n th graph, I_n denotes some quantitative indexes, such as the age, the state of education, etc., and y_n is the label of the n th graph, which is the ground-truth diagnosis for G_n . The schizophrenia diagnosis problem is thus cast as the problem of learning optimal trainable parameters θ_ϕ for a GCNN $\phi(G_n, I_n; \theta_\phi)$ that maps each graph G_n to the corresponding label y_n . The training process seeks to minimize a loss function $L = loss(\phi(G_n, I_n; \theta_\phi), y_n)$, where $loss(\cdot)$ is a cross-entropy function in this work.

The GCNN architecture has essentially two stages. In the first stage, graph features are extracted by hierarchical graph convolution and graph pooling. In the second stage, the extracted features are used in combination with other quantitative indexes to train and test a traditional neural network that outputs the predicted graph labels. In fact, the two GCNN stages are jointly and alternately optimized.

Convolutional layers in the GCNN architecture are trained to extract representative features. In this work, the graph convolution is carried on by the Chebyshev spectral graph convolution operator (ChebConv) [55]. This operator uses the Chebyshev expansion method to simplify the approximation of the graph Laplacian and repeatedly performs filtering in

the ChebConv layer. By using both node features and edge weights, useful information is extracted and learnt by the convolution layers. As well, pooling is an important operation for avoiding overfitting and reducing information redundancy and noise. In this work, graph pooling is realized by Top-KPooling [56], a pooling operation that could reduce the input graphs. For an n -node graph, the number of remaining nodes after graph pooling can be denoted as kn , where k is called the pooling ratio and $k \in (0, 1]$. These remaining nodes are selected by a learnable projection operator p . Suppose $X_{in} \in R^{n \times f}$, and $A_{in} \in R^{n \times n}$ are, respectively, the node feature and adjacency matrices, and f is the number of features for each node. Features are normalized as $z = \frac{X_{in}p}{\|p\|}$, where $\|\cdot\|$ denotes the L2 norm. The top k indexes of the selected nodes are denoted as $i = TopK(z, k)$. Hence, the remaining node features are $X_{out} = (X_{in} \otimes \tanh(z))_i$, where the symbol \otimes denotes element-wise multiplication, and $A_{out} = (A_{in})_{i,i}$. By the TopKPooling operation, nodes with the most representative features could be selected for subsequent learning steps.

After repeated graph-based operations, the resulting node features could be considered as a compressed and refined representation of the original graph. These features are then reshaped as a vector and fed to a fully-connected (FC) layer, whose output is concatenated with quantitative indexes (such as the age, the state of education, etc.) and then classified by a fully-connected neural network. The GCNN architecture adopted in this paper is shown in Fig. 1. The GCNN architecture was optimized by the Adam optimizer, with a learning rate of 5×10^{-4} , an iteration count of 700 epochs, and a ratio of the top-k pooling of 0.5. The GCNN model is essentially constructed as the traditional CNN models where the convolution and pooling are stacked alternately, in order to extract and refine useful features.

Taking into account the size of the collected dataset, training of both SVM and GNN was performed following a five-fold cross-validation scheme. That is, the data samples were divided into 5 folds. For each fold, the number of subjects from each of the three classes (FESZ, CSZ and HC) was the same. One fold (24 samples) and the other four folds (a total of 96 samples) was used for testing and training respectively. So, the training was repeated five times, and the average testing performance over these five runs was used as the result of the five-fold cross-validation scheme. Each possible feature combination was explored randomly for ten times of the five-fold cross-validation. The performance for each experiment was evaluated using four metrics: precision, recall, accuracy and F1-score [57]. To adequately demonstrate the numbers of false positives (FP) and false negatives (FN), a contingency or confusion matrix (CM) was created for each classifier. In such a matrix, elements on the diagonal are the numbers of correctly classified samples, and off-diagonal elements are the numbers of wrongly predicted samples. From the CM, the FP and FN counts of each category could be clearly displayed.

III. RESULTS

First, MMN components were extracted from EEG signals for the FESZ, CSZ and HC groups. Then, these components

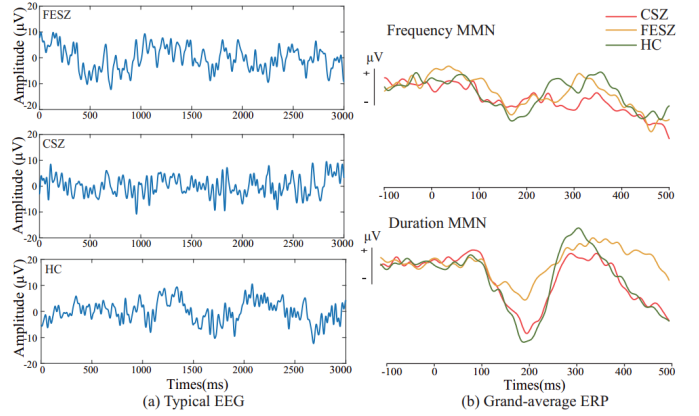


Fig. 2. Typical EEG signals and grand-average ERP waveforms of first-episode schizophrenia (FESZ), chronic schizophrenia (CSZ) and healthy control (HC).

were reconstructed using eLORETA to obtain PC-based and PLI-based brain networks at the source level. Pairwise comparisons of the brain connectivity of the three groups show significantly different connectivity ($p < 0.01$). T Graph-theoretic features of the brain networks of the FESZ, CSZ and HC groups were extracted and used for SVM classifier training and testing, while the GNN classifier was directly trained and tested on the brain networks. For each classifier and feature combination, the results of 10 repetitions of a five-fold cross-validation scheme were averaged.

Demographic characteristics and MMN amplitudes of FESZ, CSZ and HC are summarized in Table I. Typical EEG signals and grand-average event-related potential waveforms of FESZ, CSZ and HC during duration MMN and frequency MMN are shown in Fig. 2. In our work, the ERP results showed that the amplitudes of both the frequency and duration MMN had significant differences between the FESZ and CSZ groups ($p < 0.001$), and between the CS and HC groups ($p < 0.001$). There was a significant difference between the FESZ and HC groups for the duration MMN ($p = 0.048$) but not for the frequency MMN ($p = 0.269$).

For the three subject groups (FESZ, CSZ and HC), pairwise comparisons of the frequency MMN brain networks were performed. Similar comparisons were made for the duration MMN brain networks. Fig. 3 shows the significant differences in brain connectivities between group pairs for partial-correlation-based brain networks.

The results for the duration MMN showed that 29 functional connectivities were significantly different in the FESZ group compared to the HC one (Fig. 3-A1), and the main brain regions involved were the superior frontal gyrus and the medial part. The CSZ group was found to have 28 significantly different connectivities compared to the HC group (Fig. 3-A3). Involved brain regions included mainly the precentral gyrus, the media orbitofrontal cortex, the Heschl gyrus (HES), and the insula. For the FESZ and CSZ group pair during the duration MMN, 29 significantly different functional connectivities emerged (Fig. 3-A2). The main involved brain regions included the fusiform gyrus, the inferior frontal gyrus (parts triangularis), the precuneus, the superior occipital gyrus, the superior frontal gyrus, and the middle temporal gyrus.

TABLE I
DEMOGRAPHIC CHARACTERISTICS, DRUG TREATMENT AND MMN AMPLITUDES OF FIRST-EPISTODE SCHIZOPHRENIA, CHRONIC SCHIZOPHRENIA, AND HEALTHY CONTROL

Characteristic	FESZ ⁽¹⁾		CSZ ⁽²⁾		HC ⁽³⁾		Comparison		Post hoc p-values		
	N	%	N	%	N	%	χ^2	p	① vs ②	① vs ③	② vs ③
Gender(female/male)	12/28	30/70	18/23	42.5/57.5	15/25	37.5/62.5	1.364	0.506	0.245	0.478	0.648
Antipsychotic treatment											
None	24	60	4	10	-	-	-	-	-	-	-
First-generation	0	0	0	0	-	-	-	-	-	-	-
Second-generation	16	40	36	90	-	-	-	-	-	-	-
	mean	SD	mean	SD	mean	SD	F	p	① vs ②	① vs ③	② vs ③
Age(years)	25.63	6.21	28.50	5.34	26.33	5.60	2.742	0.069	0.08	1.000	0.276
Education(years)	13.40	2.87	13.88	2.62	14.48	2.91	1.476	0.233	1.000	0.267	1.000
IQ	101.48	12.403	105.58	9.732	114.1	13.345	11.667	<0.001	0.381	<0.001	0.005
Age at illness onset (years)	24.48	6.27	21.35	4.84	-	-	6.231	0.015	-	-	-
Duration of illness (months)	14.15	9.24	90.03	37.71	-	-	152.8	<0.001	-	-	-
MMN amplitudes											
Frequency MMN (μV)	-0.856	0.230	-0.570	0.210	-0.940	0.221	30.968	<0.001	<0.001	0.269	<0.001
Duration MMN (μV)	-1.637	0.480	-0.915	0.304	-1.889	0.565	47.802	<0.001	<0.001	0.048	<0.001

*FESZ: first-episode schizophrenia; CSZ: chronic schizophrenia; HC: healthy control; IQ: intelligence quotient.

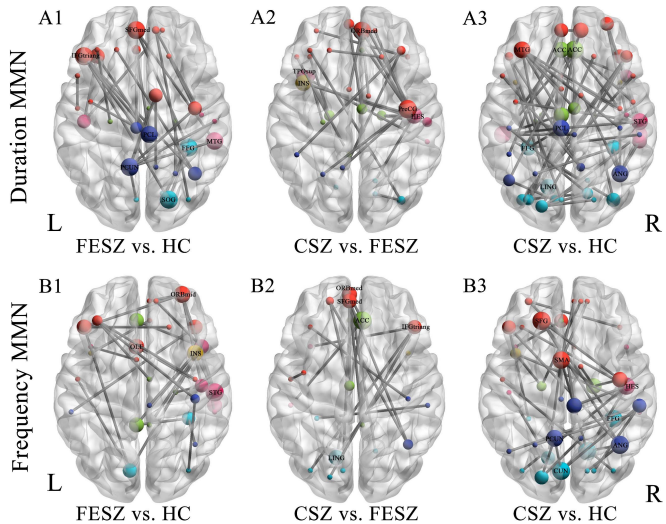


Fig. 3. The significantly different connectivities ($p < 0.01$) between brain regions during the frequency and duration MMN for pairs of first-episode schizophrenia (FESZ), chronic schizophrenia (CSZ) and healthy control (HC). The size of a node is directly proportional to its betweenness centrality. The brain areas are represented by different node colors: red for the frontal lobe and central region; fuchsia for the temporal lobe; mazarine blue for parietal lobe; wathet for the occipital lobe; yellow for the insula; green for limbic lobe. The brain networks A1-A3 are built for the duration MMN while the B1-B3 ones are for the frequency MMN. The detail parallelism between abbreviations and the corresponding brain regions is given in Supplementary Table A.2. The connectivities was displayed by BrainNet Viewer (<http://www.nitrc.org/projects/bnv/>).

The results for the frequency MMN showed that there were 17 functional connectivities with statistically significant differences between the FESZ and HC groups (as shown in Fig. 3-B1) and the functional connectivities of the FESZ group were generally weaker than those of the HC group. The most relevant brain regions were the anterior cingulate cortex, the media orbitofrontal cortex, the lingual gyrus, the superior frontal gyrus, and the inferior frontal gyrus (parts triangularis). Compared with the HC group, the CSZ group had 62 significantly different functional connectivities (Fig. 3-B3),

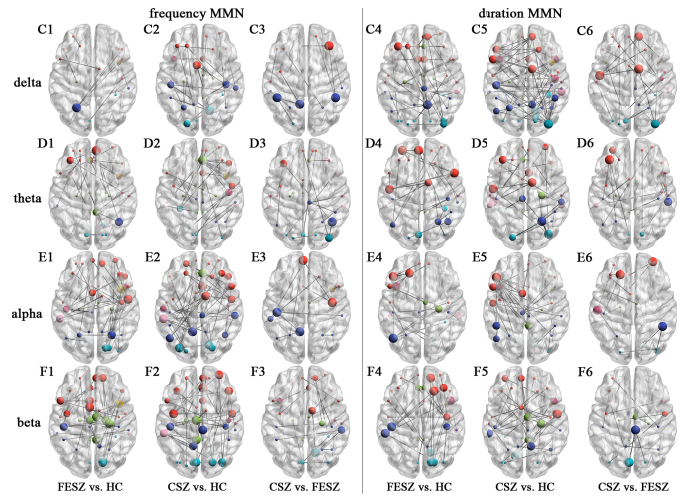


Fig. 4. The significantly different connectivities of brain networks constructed by the phase lag index during the frequency and duration MMN of delta, theta, alpha and beta band for pairwise comparisons of first-episode schizophrenia (FESZ), chronic schizophrenia (CSZ), and healthy control (HC).

and the involved regions included parts of the temporal lobe (such as the inferior, superior, and middle temporal gyri, as well as the fusiform gyrus), the frontal lobe (the superior and middle frontal gyri), the anterior cingulate cortex, the angular gyrus, and the lingual gyrus. Compared with the CSZ group, the FESZ group had 30 significantly different connectivities among brain regions during the frequency MMN as shown in Fig. 3-B2. The involved brain regions were mainly the temporal lobe (the inferior, superior, and middle temporal gyri, as well as the temporal pole, and the fusiform gyrus), the frontal lobe (the middle and inferior frontal gyri, the orbital part, and the parts triangularis), the insula, and the limbic lobe (the olfactory gyrus, as well as the anterior and posterior cingulate cortex).

More detailed information of the regions in Fig. 3 is shown in the appendix, in which regions involved in the top

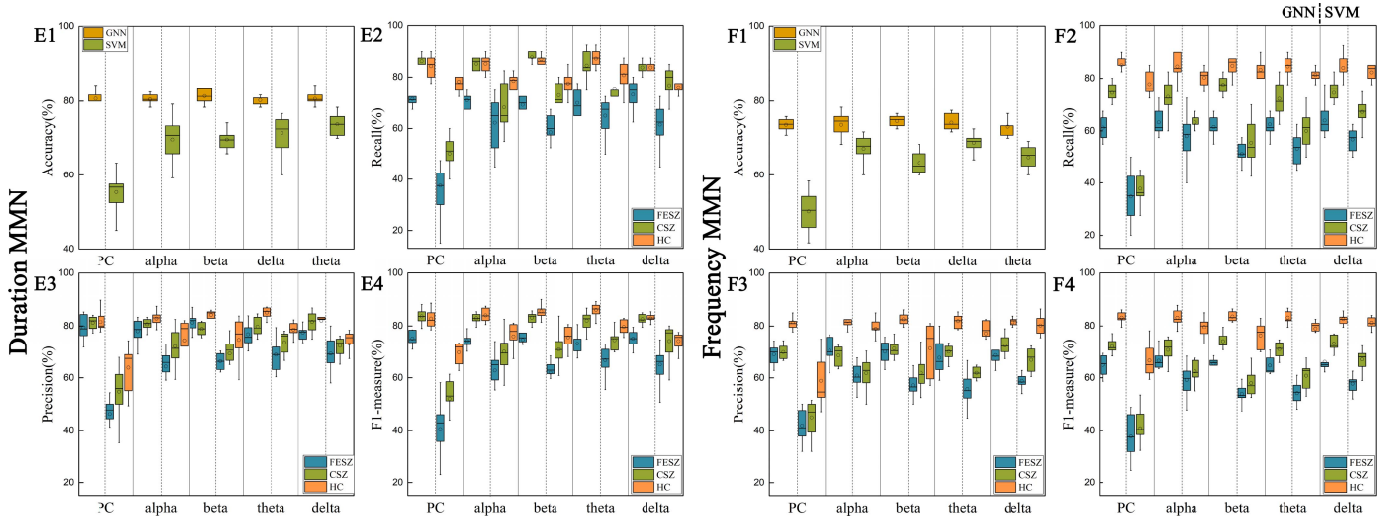


Fig. 5. Results of four performance indicators (accuracy, recall, precision and F1-score) for classifying the FESZ, CSZ, and HC patterns by the GNN and SVM classifiers, respectively. Charts for the GNN and SVM classification results are shown on the left and right sides of each dashed line, respectively. PC: partial correlation; FESZ: first-episode schizophrenia; CSZ: chronic schizophrenia; HC: healthy control.

TABLE II

ACCURACY (%) FOR CLASSIFYING FIRST-EPISEDE SCHIZOPHRENIA, CHRONIC SCHIZOPHRENIA AND HEALTHY SUBJECTS BY SVM AND GNN CLASSIFIERS

Method	Stimulant	PC	alpha	beta	theta	delta
SVM	dMMN	55.33±5.26	69.67±5.74	69.67±4.14	66.58±1.82	71.42±5.12
	fMMN	50.08±5.42	67.17±4.09	63.33±2.91	64.83±3.11	68.75±2.30
GNN	dMMN	80.67±2.00	80.50±1.43	81.33±1.81	80.58±2.39	80.25±1.25
	fMMN	73.58±1.67	73.58±3.07	74.58±1.53	73.08±2.36	74.17±2.19

*dMMN: duration MMN; fMMN: frequency MMN; PC: partial correlation.

35 significantly different connectivities according to P-value from large to small between CSZ and HC based on duration MMN are shown in appendices Table A.3. And all regions involved in Fig.3 are shown in appendices Table A.4 according to the betweenness centrality from large to small.

Fig. 4 shows the significantly different connectivities of the brain networks, which were constructed by measuring the phase lag index between the brain regions during the frequency and duration MMN of the delta, theta, alpha and beta bands for pairwise comparisons of the FESZ, CSZ and HC groups.

For different frequency bands and deviant stimuli, the following trend consistently occurs for the number of significantly different connectivities between groups: CSZ vs. HC > FESZ vs. HC < CSZ vs. FESZ. In other words, the FESZ and CSZ groups have more significantly different connectivities than the HC one. This suggests a large difference in the brain functions between schizophrenia patients and healthy subjects. The CSZ-versus-HC group pair has the largest number of significantly different connectivities in the delta band of the duration MMN, which involves a wide range of brain regions that diffuse throughout the cerebral cortex (See Fig. 4-C5). The FESZ-versus-HC group pair has larger numbers of significantly different connectivities in the following cases compared to other cases: the alpha and beta bands in the frequency MMN, and the delta band

in the duration MMN. The number of significantly different connectivities for the CSZ-and-FESZ pair is small compared to the other two pairs.

For each experimental configuration, ten test runs were performed with a 5-fold cross-validation scheme. The classification results were recorded and evaluated using the accuracy, recall, precision, and F1-score, as summarized in Fig. 5. The specific values of these features are shown in Table A.5-8 of *Supplementary Materials*.

The GNN classification accuracy was statistically significantly higher ($p < 0.001$) than that using SVM for all experimental configurations. The average and the standard deviation of the accuracy for each configuration are given in Table II. The highest-accuracy configuration is the GNN one in which brain networks are constructed based on the delta band of the duration MMN. Nevertheless, GNN-based results for other frequency bands of the duration MMN also provided comparable performance outcomes that exceed those of the partial-correlation networks.

From the performance under different deviant stimuli signals, the classification results based on the duration MMN are consistently higher than those based on the frequency MMN. In addition to the accuracy, the other three performance indicators (recall, precision, and F1-score) show similar trends for the experimental configurations.

The CM results of the SVM and GNN for classifying the FESZ, CSZ and HC are demonstrated in Fig.6. The numbers in each CM are obtained by summing the results of 10 repetitions of 5-fold cross-validation experiments. Figure 6 shows that the performance of the GNN algorithm is better than that of the SVM one for both the duration and frequency deviant stimuli. The GNN classifier with duration MMN shows better performance than that with frequency MMN under the same conditions.

IV. DISCUSSION

In this study, functional brain networks based on MMN signals were first constructed for the FESZ, SCZ and HC

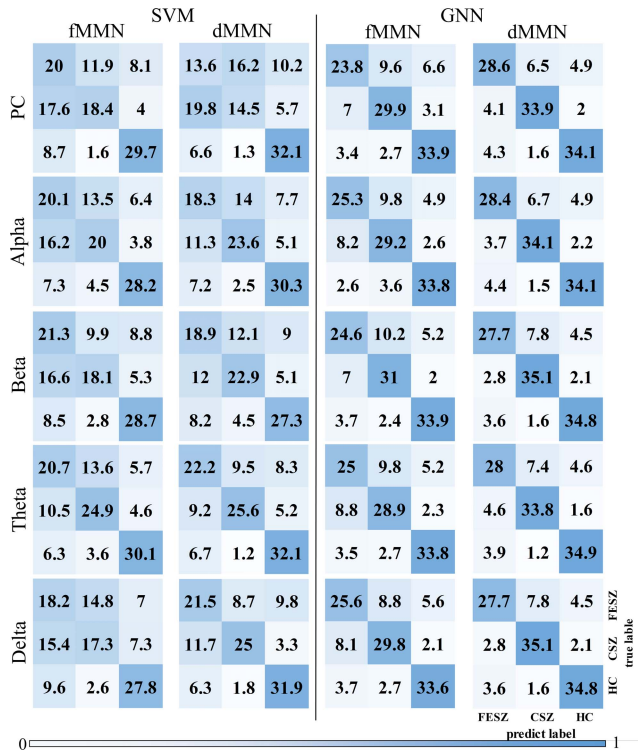


Fig. 6. Confusion matrixes as results of 10 times repeated 5-fold cross-validation experiments for classifying schizophrenia (FESZ), chronic schizophrenia (CSZ) and healthy control (HC) by the GNN and SVM classifiers, respectively. In each confusion matrix, the row represents true labels and the column represents predict labels. To be specific, the row of confusion matrix contains 40 true samples of one class (5 × 8 test samples in each 5-fold cross-validation). dMMN: duration MMN; fMMN: frequency MMN; PC: partial correlation.

groups. The groups can be differentiated by differences in connectivity patterns for the constructed networks. A novel GNN classifier was trained on the brain network structures to identify the FESZ and CSZ groups and distinguish them from the HC one. Alternatively, the SVM classifiers were trained on graph-theoretic features of the brain networks. In addition, differences in connectivities between regions were examined in four frequency bands (theta, beta, alpha and delta) and two types of deviant stimuli among pairs of the FESZ, CSZ and HC groups.

The trend of the differences between groups is consistently shown in the ERP components and the partial-correlation-based brain networks. For the frequency MMN, the damage of the connections between brain regions in the CSZ group is more severe than that in the FESZ group. The CSZ group has a higher number of connections compared to the FESZ and HC groups. This intuitively shows that the CSZ group exhibits a strong contrast with the other two groups for the frequency MMN. The results also suggest that the impaired brain functions in the CSZ group are significantly more severe than those in the FESZ group. This conclusion is consistent with earlier work based on resting-state magnetic resonance imaging (MRI) [58] and resting-state functional MRI [23]. Moreover, the disease progression is an important source of heterogeneity in patients with schizophrenia [59]. From the

results of the MMN-induced brain functional connectivities between groups (Fig. 3), the FESZ and CSZ groups show significant differences in connectivity for both the frequency MMN and the duration MMN. These connectivity differences are due to differences in the brain functions between the two groups. Which explains the larger effect size of MMN amplitude in the diagnosis of CSZ than that in FESZ (Table A.9 in *Supplementary Materials*) [60].

We also found that the MMN damage in the FESZ and CSZ groups was associated with the auditory cortex. A previous study [61] has found that the human auditory cortex consists of primary and secondary regions, where the primary auditory cortex is located in the posterior third of the Heschl gyrus, while the secondary auditory cortex spans a part of the HES in addition to the posterior part of the superior temporal gyrus (STG). It has also been found that the auditory cortex of schizophrenic subjects may be impaired during adolescence [62]. The results of this study show that both the frequency MMN and duration MMN in the FESZ case were negatively impacted in the STG and HES regions, respectively. This indicated that the auditory MMN also requires the auditory cortex for information processing. Indeed, MMN was found to be dependent on the auditory cortex to create and maintain short-term auditory memory based on repeated standard stimuli, and then detect deviations from regular patterns due to deviant stimuli [63]–[65]. This capability of the auditory cortex is called the “primary auditory memory,” which was found to be based on the N-methyl-D-aspartate receptor (NMDAR-like) false prediction response of the auditory cortex [64], [66]–[68]. Zoological studies [69] have also confirmed that auditory MMN occurs in the auditory cortex. Besides, there is a relationship between MMN damage and auditory cortex dysfunction in schizophrenic subjects. A brain structural imaging study [70] has also found that MMN damage in patients with schizophrenia is associated with thinning of the STG part of the auditory cortex.

By observing brain networks during MMN, we can realize that dysfunction occurs in the frontal lobe for both FESZ and CSZ groups compared with the healthy group. This shows that in the early stages of the schizophrenia process (i.e. FESZ stage) impairment of the frontal lobe has begun to emerge. Consistent conclusions are obtained from earlier studies. [4] This indicates that the frontal lobe damage is a consistent schizophrenia indicator that could be exploited for early diagnosis.

Some areas out of the auditory cortex were observed in this study. In duration MMN of FESZ and frequency MMN of CSZ, fusiform gyrus was found to involve a large number of abnormal connectivities. It was also reported a decreased duration MMN current density of fusiform in FESZ by [71] and reduced MRI volumes of the fusiform gyrus in CSZ by [72]. Precuneus, superior occipital gyrus, anterior cingulate cortex and angular gyrus showed abnormality in this study, which was reported with reduced current source density in MMN of schizophrenia by a previous study [73]. In this study, we also found abnormal insula in the frequency of FESZ, which was showed gray matter volume abnormalities in FESZ [25]. The lingual gyrus has not been reported related to

TABLE III
A COMPARATIVE ANALYSIS REPORT FOR OUR PROPOSED METHOD WITH THE EXISTING METHODS

Author	Dataset	EEG	Features extraction	Classifier	ACC
Santos-Mayo et al. [29]	16 SZ patients and 31 HC subjects	P300	Time and frequency domain features	MLP	93.42%
Shim et al. [30]	34 SZ patients and 34 HC subjects	P300	Sensor level and source level features	SVM	88.24%
Khare et al. [31]	49 SZ patients and 32 HC subjects	Press button task	Empirical wavelet transform	SVM	88.7%
Siuly et al. [32]	49 SZ patients and 32 HC subjects	Press button task	Empirical mode decomposition	EBT	89.59%
Johannesen et al. [33]	40 SZ patients and 12 HC subjects	Working memory	Rhythms separated using filtering	SVM	87%
Kim et al. [34]	90 SZ patients and 90 HC subjects	Resting-state	Spectral analysis in five frequency bands	ROC	62.2%
Krishnan et al. [35]	14 SZ patients and 14 HC subjects	Resting-state	Multivariate empirical mode decomposition	SVM	93%
Das et al. [36]	14 SZ patients and 14 HC subjects	Resting-state	Multivariate iterative filtering	SVM	98.9%
Boostani et al. [37]	13 SZ patients and 18 HC subjects	Resting-state	Autoregressive model parameters, band power and fractal dimension	LDA	87.51%
Kim et al. [38]	119 SZ patients and 119 HC subjects	Resting-state	Brain network features	LDA	80.66%
Phang et al. [39]	45 SZ patients and 39 HC subjects	Resting-state	Brain connectivity networks	CNN	91.69%
Khare et al. [40]	49 SZ patients and 32 HC subjects	press button task	Smoothed pseudo-Wigner Ville distribution	CNN	93.36%
Our proposed method	80 SZ patients and 40 HC subjects	MMN	Brain network	GNN	93.33%
	40 FESZ, 40 UHR and 40 HC subjects	MMN	Brain network	GNN	84.17%

* ACC: accuracy; SZ: schizophrenia; MLP: multilayer perceptron; EBT: ensemble bagged tree; ROC: receiver operating characteristic.

MMN in schizophrenia, but a significantly increased gyration was observed in FESZ in a right parahippocampal–lingual cortex area [74].

The brain network classification results during auditory MMN differ slightly according to whether the partial correlation or the PLI method is used. On the one hand, the measurement of the time-domain partial correlation between two nodes is different from that of the PLI assessment which examines the frequency-domain characteristics. On the other hand, the partial correlation uses the full frequency band of a signal, while the PLI method exploits frequency subbands. The ERP is believed to be a superimposition of single-trial oscillations with alpha, beta, theta, delta and gamma rhythms [75], resulting in information hiding, and lack of information details for the full frequency band. However, both partial correlation and PLI methods show different strengths in identifying large areas of damage in the brain regions of schizophrenic patients. Practically, any of the two methods or hybrid methods may be considered.

The GNN classifier shows superior improvements in the accuracy, recall, precision, F1-score and confusion matrix in comparison to the SVM classifier. This indicates that the combination of GNN and brain networks brings better performance than classical classifiers. This improvement can be clearly attributed to the superiority of GNN on feature extraction. Considering the training of the SVM, features that are taken as the input of the SVM are manually selected based on previous understanding of the brain network. These features may not enough in schizophrenia classification. The GNN, however, could extract enough and useful features for classification through the back-propagation approach. So that enough and useful features could be extracted automatically during training. Since the quality of the features is usually the key to determine the performance of algorithms, the superior feature extraction capability makes the GNN have better performance.

Another prominent improvement factor is that the deeply cascaded structure of the GNN is helpful to learn the high-level combination of the features. The deep structure of the GNN

could take the interrelationship among different nodes and edges of the graph into consideration, so that the complex relationship underneath and the joint effort of different brain regions may be discovered. This kind of high-level relationship may be difficult to be described by formulas, but could be represented by the non-linear combination of multiple layers in GNN, and contribute to the final performance of the algorithm.

The highest accuracy of the classifications reached 84.17% in a single trial five-fold cross-validation test, and the average of the random ten times five-fold cross-validation test reached a maximum of 81.33%, both of which were performed by GNN. Potential classifier inputs were the brain networks as well as other features including the MCCB cognitive scores, demographic characteristics, and electrophysiological MMN features (i.e. the amplitude and the latency). The experimental results with brain network inputs only returned a lower accuracy compared to the case when the brain networks were combined with MCCB features. In addition, we analyze the results of CZ and HC classifications in this study and compare our proposed method with the existing methods in the Table III. Our proposed method yields an accuracy of 93.33%. In summary, these demonstrate the importance of augmenting the brain connectivity features with other relevant features to more accurately identify schizophrenic subjects and distinguish them from healthy ones.

In this paper, the experimental configuration with the highest accuracy is the one in which a GNN classifier is used with an input of brain networks constructed based on the delta-frequency band of the duration MMN. For low-frequency MMN oscillations (<40Hz), a related study [76] found that the delta-frequency band showed the strongest correlation with the MMN of schizophrenia. This result is consistent with our results. Also, as shown in Fig. 4, the PLI values of the delta-band brain regions of the HC and CSZ groups are obviously higher than those in the other frequency bands, while the PLI values of the brain regions for the FESZ group are relatively low. Therefore, the delta-band features can separate the three groups more effectively compared to features of other frequency bands.

The deviant stimulus type also affects the classification performance. Classifiers based on the duration MMN achieved higher accuracies than the frequency MMN ones. This conclusion is supported by the results of many studies [7], [11] which have consistently shown that the duration MMN is indeed more robust than the frequency MMN in differentiating schizophrenic and healthy subjects. The MMN performance and brain functional connectivity results in our study were also consistent with the MMN latency and amplitude results of [46].

V. CONCLUSION

In this work, we investigated the brain functional connectivities underlying the duration and frequency MMN among the FESZ, CSZ and HC groups. Graph neural networks (GNN) were applied to MMN-based brain functional networks for the classification of schizophrenia patients and healthy subjects. Besides, graph-theoretic local and global features were extracted from brain networks and used to train a SVM for classifying the three groups. In conclusion, the significantly different functional connectivities between the CSZ and HC groups showed more extensively involved brain regions in comparison to the FESZ-and-HC group pair. The GNN classifier trained on the brain functional networks achieved an accuracy of 84.17%, significantly outperforming the SVM classifier trained on graph-theoretic features (which had a maximal accuracy of only 69.17%). This demonstrates that GNN classifiers trained on EEG-based functional networks can provide clinically-applicable high classification performance for the FESZ, CSZ and HC groups. For future work, MMN-based brain networks of ultra-high-risk individuals shall be exploited towards achieving early schizophrenia diagnosis and intervention. On the other hand, dynamic brain networks could be constructed to explore more effective features for schizophrenia diagnosis.

REFERENCES

- [1] T. E. Goldberg *et al.*, "Cognitive improvement after treatment with second-generation antipsychotic medications in first-episode schizophrenia: Is it a practice effect?" *Arch. Gen. Psychiatry*, vol. 64, no. 10, pp. 1115–1122, Oct. 2007.
- [2] R. Näätänen, "The mismatch negativity: A powerful tool for cognitive neuroscience," *Ear Hearing*, vol. 16, no. 1, pp. 6–18, Feb. 1995.
- [3] M. F. Green *et al.*, "Perception measurement in clinical trials of schizophrenia: Promising paradigms from CNTRICS," *Schizophrenia Bull.*, vol. 35, no. 1, pp. 163–181, Jan. 2009.
- [4] D. F. Hermens, P. B. Ward, M. A. R. Hodge, M. Kaur, S. L. Naismith, and I. B. Hickie, "Impaired MMN/P3a complex in first-episode psychosis: Cognitive and psychosocial associations," *Prog. Neuropsychopharmacol. Biol. Psychiatry*, vol. 34, no. 6, pp. 822–829, Aug. 2010.
- [5] A. Mondragón-Maya *et al.*, "Reduced P3a amplitudes in antipsychotic naïve first-episode psychosis patients and individuals at clinical high-risk for psychosis," *J. Psychiatric Res.*, vol. 47, no. 6, pp. 755–761, Jun. 2013.
- [6] D. F. Salisbury, M. E. Shenton, C. B. Griggs, A. Bonner-Jackson, and R. W. McCarley, "Mismatch negativity in chronic schizophrenia and first-episode schizophrenia," *Arch. Gen. Psychiatry*, vol. 59, no. 8, pp. 686–694, Aug. 2002.
- [7] E. Magno, S. Yeap, J. H. Thakore, H. Garavan, P. De Sanctis, and J. J. Foxe, "Are auditory-evoked frequency and duration mismatch negativity deficits endophenotypic for schizophrenia? High-density electrical mapping in clinically unaffected first-degree relatives and first-episode and chronic schizophrenia," *Biol. Psychiatry*, vol. 64, no. 5, pp. 385–391, Sep. 2008.
- [8] Y. Higuchi, T. Seo, T. Miyanishi, Y. Kawasaki, M. Suzuki, and T. Sumiyoshi, "Mismatch negativity and P3a/reorienting complex in subjects with schizophrenia or at-risk mental state," *Frontiers Behav. Neurosci.*, vol. 8, p. 172, May 2014.
- [9] V. B. Perez *et al.*, "Automatic auditory processing deficits in schizophrenia and clinical high-risk patients: Forecasting psychosis risk with mismatch negativity," *Biol. Psychiatry*, vol. 75, no. 6, pp. 459–469, Mar. 2014.
- [10] R. Näätänen and I. Winkler, "The concept of auditory stimulus representation in cognitive neuroscience," *Psychol. Bulletin*, vol. 125, no. 6, p. 826, Nov. 1999.
- [11] D. F. Salisbury, N. R. Polizzotto, P. G. Nestor, S. M. Haigh, J. Koehler, and R. W. McCarley, "Pitch and duration mismatch negativity and premorbid intellect in the first hospitalized schizophrenia spectrum," *Schizophrenia Bull.*, vol. 43, no. 2, pp. 407–416, Mar. 2017.
- [12] P. T. Michie *et al.*, "Duration and frequency mismatch negativity in schizophrenia," *Clin. Neurophysiol.*, vol. 111, no. 6, pp. 1054–1065, Jun. 2000.
- [13] M. H. Giard *et al.*, "Separate representation of stimulus frequency, intensity, and duration in auditory sensory memory: An event-related potential and dipole-model analysis," *J. Cognit. Neurosci.*, vol. 7, no. 2, pp. 133–143, Apr. 1995.
- [14] B. Jemel, C. Achenbach, B. W. Müller, B. Röpcke, and R. D. Oades, "Mismatch negativity results from bilateral asymmetric dipole sources in the frontal and temporal lobes," *Brain Topogr.*, vol. 15, no. 1, pp. 13–27, Sep. 2002.
- [15] T. Rinne *et al.*, "Scalp-recorded optical signals make sound processing in the auditory cortex visible?" *NeuroImage*, vol. 10, no. 5, pp. 620–624, Nov. 1999.
- [16] M.-H. Giard, F. Perrin, J. Pernier, and P. Bouchet, "Brain generators implicated in the processing of auditory stimulus deviance: A topographic event-related potential study," *Psychophysiology*, vol. 27, no. 6, pp. 627–640, Nov. 1990.
- [17] E. Yago, M. J. Corral, and C. Escera, "Activation of brain mechanisms of attention switching as a function of auditory frequency change," *Neuroreport*, vol. 12, no. 18, pp. 4093–4097, Dec. 2001.
- [18] E. Yago, C. Escera, K. Alho, and M.-H. Giard, "Cerebral mechanisms underlying orienting of attention towards auditory frequency changes," *Neuroreport*, vol. 12, no. 11, pp. 2583–2587, Aug. 2001.
- [19] K. J. Friston, "Models of brain function in neuroimaging," *Annu. Rev. Psychol.*, vol. 56, no. 1, pp. 57–87, Feb. 2005.
- [20] N. Fogelson, V. Litvak, A. Peled, M. Fernandez-del-Olmo, and K. Friston, "The functional anatomy of schizophrenia: A dynamic causal modeling study of predictive coding," *Schizophrenia Res.*, vol. 158, nos. 1–3, pp. 204–212, Sep. 2014.
- [21] M. R. Dauvermann *et al.*, "Computational neuropsychiatry-schizophrenia as a cognitive brain network disorder," *Frontiers Psychiatry*, vol. 5, p. 30, Mar. 2014.
- [22] R. W. Heinrichs and K. K. Zakzanis, "Neurocognitive deficit in schizophrenia: A quantitative review of the evidence," *Neuropsychology*, vol. 12, no. 3, pp. 426–445, Jul. 1998.
- [23] T. Li *et al.*, "Brain-wide analysis of functional connectivity in first-episode and chronic stages of schizophrenia," *Schizophrenia Bull.*, vol. 43, no. 2, pp. 436–448, Mar. 2017.
- [24] W. Pettersson-Yeo, P. Allen, S. Benetti, P. McGuire, and A. Mechelli, "Dysconnectivity in schizophrenia: Where are we now?" *Neurosci. Biobehavioral Rev.*, vol. 35, no. 5, pp. 1110–1124, Apr. 2011.
- [25] S.-H. Lee *et al.*, "Initial and progressive gray matter abnormalities in insular gyrus and temporal pole in first-episode schizophrenia contrasted with first-episode affective psychosis," *Schizophrenia Bull.*, vol. 42, no. 3, pp. 790–801, May 2016.
- [26] D. Dima, S. Frangou, L. Burge, S. Braeutigam, and A. C. James, "Abnormal intrinsic and extrinsic connectivity within the magnetic mismatch negativity brain network in schizophrenia: A preliminary study," *Schizophrenia Res.*, vol. 135, nos. 1–3, pp. 23–27, Mar. 2012.
- [27] D. Koshiyama *et al.*, "Abnormal effective connectivity underlying auditory mismatch negativity impairments in schizophrenia," *Biol. Psychiatry. Cognit. Neurosci. Neuroimaging*, vol. 5, no. 11, pp. 1028–1039, Nov. 2020.
- [28] T. Rosburg, "Left hemispheric dipole locations of the neuromagnetic mismatch negativity to frequency, intensity and duration deviants," *Cognit. Brain Res.*, vol. 16, no. 1, pp. 83–90, Mar. 2003.
- [29] L. Santos-Mayo, L. M. San-Jose-Revuelta, and J. I. Arribas, "A computer-aided diagnosis system with EEG based on the P3b wave during an auditory odd-ball task in schizophrenia," *IEEE Trans. Biomed. Eng.*, vol. 64, no. 2, pp. 395–407, Feb. 2017.

- [30] M. Shim, H.-J. Hwang, D.-W. Kim, S.-H. Lee, and C.-H. Im, "Machine-learning-based diagnosis of schizophrenia using combined sensor-level and source-level EEG features," *Schizophrenia Res.*, vol. 176, nos. 2–3, pp. 314–319, 2016.
- [31] S. K. Khare, V. Bajaj, S. Siuly, and G. Sinha, *Classification of Schizophrenia Patients Through Empirical Wavelet Transformation Using Electroencephalogram Signals*. Bristol, U.K.: IOP Publishing, 2020.
- [32] S. Siuly, S. K. Khare, V. Bajaj, H. Wang, and Y. Zhang, "A computerized method for automatic detection of schizophrenia using EEG signals," *IEEE Trans. Neural Syst. Rehabil. Eng.*, vol. 28, no. 11, pp. 2390–2400, Nov. 2020.
- [33] J. K. Johannessen, J. Bi, R. Jiang, J. G. Kenney, and C.-M.-A. Chen, "Machine learning identification of EEG features predicting working memory performance in schizophrenia and healthy adults," *Neuropsychiatric Electrophysiol.*, vol. 2, no. 1, p. 3, Feb. 2016.
- [34] J. W. Kim, Y. S. Lee, D. H. Han, K. J. Min, J. Lee, and K. Lee, "Diagnostic utility of quantitative EEG in un-medicated schizophrenia," *Neurosci. Lett.*, vol. 589, pp. 126–131, Mar. 2015.
- [35] P. T. Krishnan, A. N. J. Raj, P. Balasubramanian, and Y. Chen, "Schizophrenia detection using MultivariateEmpirical mode decomposition and entropy measures from multichannel EEG signal," *Biocybernetics Biomed. Eng.*, vol. 40, no. 3, pp. 1124–1139, Jul. 2020.
- [36] K. Das and R. B. Pachori, "Schizophrenia detection technique using multivariate iterative filtering and multichannel EEG signals," *Biomed. Signal Process. Control*, vol. 67, May 2021, Art. no. 102525.
- [37] R. Boostani, K. Sadatnezhad, and M. Sabeti, "An efficient classifier to diagnose of schizophrenia based on the EEG signals," *Expert Syst. Appl.*, vol. 36, no. 3, pp. 6492–6499, Apr. 2009.
- [38] J.-Y. Kim, H. S. Lee, and S.-H. Lee, "EEG source network for the diagnosis of schizophrenia and the identification of subtypes based on symptom severity—A machine learning approach," *J. Clin. Med.*, vol. 9, no. 12, p. 3934, Dec. 2020.
- [39] C.-R. Phang, F. Noman, H. Hussain, C.-M. Ting, and H. Ombao, "A multi-domain connectome convolutional neural network for identifying schizophrenia from EEG connectivity patterns," *IEEE J. Biomed. Health Informat.*, vol. 24, no. 5, pp. 1333–1343, May 2020.
- [40] S. K. Khare, V. Bajaj, and U. R. Acharya, "SPWVD-CNN for automated detection of schizophrenia patients using EEG signals," *IEEE Trans. Instrum. Meas.*, vol. 70, pp. 1–9, 2021.
- [41] F. Scarselli, M. Gori, A. C. Tsoi, M. Hagenbuchner, and G. Monfardini, "The graph neural network model," *IEEE Trans. Neural Netw.*, vol. 20, no. 1, pp. 61–80, Jan. 2009.
- [42] J. Bruna, W. Zaremba, A. Szlam, and Y. LeCun, "Spectral networks and locally connected networks on graphs," 2013, *arXiv:1312.6203*. [Online]. Available: <http://arxiv.org/abs/1312.6203>
- [43] F. Scarselli, S. L. Yong, M. Gori, M. Hagenbuchner, A. C. Tsoi, and M. Maggini, "Graph neural networks for ranking web pages," in *Proc. IEEE/WIC/ACM Int. Conf. Web Intell.*, Sep. 2005, pp. 666–672.
- [44] S. L. Yong, M. Hagenbuchner, A. C. Tsoi, F. Scarselli, and M. Gori, "Document mining using graph neural network," in *Proc. 5th Int. Workshop Initiative Eval. XML Retr.*, Dec. 2006, pp. 458–472.
- [45] L. Di Noi, M. Hagenbuchner, F. Scarselli, and A. C. Tsoi, "Web spam detection by probability mapping graphsoms and graph neural networks," in *Proc. Int. Conf. Artif. Neural Netw.*, Sep. 2010, pp. 372–381.
- [46] Y.-B. Xiong, Q.-J. Bo, C.-M. Wang, Q. Tian, Y. Liu, and C.-Y. Wang, "Differential of frequency and duration mismatch negativity and theta power deficits in first-episode and chronic schizophrenia," *Frontiers Behav. Neurosci.*, vol. 13, p. 37, Mar. 2019.
- [47] C. Andreou *et al.*, "Resting-state theta-band connectivity and verbal memory in schizophrenia and in the high-risk state," *Schizophrenia Res.*, vol. 161, nos. 2–3, pp. 299–307, Feb. 2015.
- [48] L. Canuet *et al.*, "Resting-state EEG source localization and functional connectivity in schizophrenia-like psychosis of epilepsy," *PLoS ONE*, vol. 6, no. 11, Nov. 2011, Art. no. e27863.
- [49] C. Andreou *et al.*, "Increased resting-state gamma-band connectivity in first-episode schizophrenia," *Schizophrenia Bull.*, vol. 41, no. 4, pp. 930–939, Jul. 2015.
- [50] S. S. Keerthi and C.-J. Lin, "Asymptotic behaviors of support vector machines with Gaussian kernel," *Neural Comput.*, vol. 15, no. 7, pp. 1667–1689, Mar. 2003.
- [51] L. C. Freeman, "A set of measures of centrality based on betweenness," *Sociometry*, vol. 40, pp. 35–41, Mar. 1977.
- [52] A. Bavelas, "Communication patterns in task-oriented groups," *J. Acoust. Soc. Amer.*, vol. 22, no. 6, pp. 725–730, Jun. 1950.
- [53] K. G. Jöreskog, "Testing a simple structure hypothesis in factor analysis," *Psychometrika*, vol. 31, no. 2, pp. 165–178, Jun. 1966.
- [54] A. Krizhevsky, I. Sutskever, and G. E. Hinton, "ImageNet classification with deep convolutional neural networks," *Commun. ACM*, vol. 60, no. 6, pp. 84–90, May 2017.
- [55] M. Defferrard, X. Bresson, and P. Vandergheynst, "Convolutional neural networks on graphs with fast localized spectral filtering," in *Proc. Adv. Neural Inf. Process. Syst.*, vol. 29, D. D. Lee, M. Sugiyama, U. V. Luxburg, I. Guyon and R. Garnett, Eds., 2016, pp. 3844–3852.
- [56] C. Cangea, P. Veličković, N. Jovanović, T. Kipf, and P. Liò, "Towards sparse hierarchical graph classifiers," 2018, *arXiv:1811.01287*. [Online]. Available: <http://arxiv.org/abs/1811.01287>
- [57] D. M. W. Powers, "Evaluation: From precision, recall and F-measure to ROC, informedness, markedness and correlation," Oct. 2020, *arXiv:2010.16061*. [Online]. Available: <http://arxiv.org/abs/2010.16061>
- [58] M. Lee *et al.*, "Neural mechanisms of mismatch negativity dysfunction in schizophrenia," *Mol. Psychiatry*, vol. 22, no. 11, p. 1585, Feb. 2017.
- [59] P. Fusar-Poli, P. Allen, and P. McGuire, "Neuroimaging studies of the early stages of psychosis: A critical review," *Eur. Psychiatry*, vol. 23, no. 4, pp. 237–244, Jun. 2008.
- [60] M. A. Erickson, A. Ruffle, and J. M. Gold, "A meta-analysis of mismatch negativity in schizophrenia: From clinical risk to disease specificity and progression," *Biol. Psychiatry*, vol. 79, no. 12, pp. 980–987, Jun. 2016.
- [61] R. A. Sweet, K.-A. Dorph-Petersen, and D. A. Lewis, "Mapping auditory core, lateral belt, and parabelt cortices in the human superior temporal gyrus," *J. Comparative Neurol.*, vol. 491, no. 3, pp. 270–289, Oct. 2005.
- [62] J. Hill, T. Inder, J. Neil, D. Dierker, J. Harwell, and D. Van Essen, "Similar patterns of cortical expansion during human development and evolution," *Proc. Nat. Acad. Sci. USA*, vol. 107, no. 29, pp. 13135–13140, Jul. 2010.
- [63] M. I. Garrido, K. J. Friston, S. J. Kiebel, K. E. Stephan, T. Baldeweg, and J. M. Kilner, "The functional anatomy of the MMN: A DCM study of the roving paradigm," *NeuroImage*, vol. 42, no. 2, pp. 936–944, Aug. 2008.
- [64] M. I. Garrido, J. M. Kilner, K. E. Stephan, and K. J. Friston, "The mismatch negativity: A review of underlying mechanisms," *Clin. Neurophysiol.*, vol. 120, no. 3, pp. 453–463, Mar. 2009.
- [65] R. Näätänen, M. Tervaniemi, E. Sussman, P. Paavilainen, and I. Winkler, "'Primitive intelligence' in the auditory cortex," *Trends Neurosci.*, vol. 24, no. 5, pp. 283–288, May 2001.
- [66] K. Friston, "A theory of cortical responses," *Philos. Trans. Roy. Soc. London B, Biol. Sci.*, vol. 360, no. 1456, pp. 815–836, Apr. 2005.
- [67] J. Todd, P. T. Michie, U. Schall, P. B. Ward, and S. V. Catts, "Mismatch negativity (MMN) reduction in schizophrenia—Impaired prediction-error generation, estimation or salience?" *Int. J. Psychophysiol.*, vol. 83, no. 2, pp. 222–231, Feb. 2012.
- [68] C. Wacongne, J.-P. Changeux, and S. Dehaene, "A neuronal model of predictive coding accounting for the mismatch negativity," *J. Neurosci.*, vol. 32, no. 11, pp. 3665–3678, Mar. 2012.
- [69] T. I. Shiramatsu and H. Takahashi, "Mismatch negativity in rat auditory cortex represents the empirical salience of sounds," *Frontiers Neurosci.*, vol. 12, p. 924, Dec. 2018.
- [70] S. Kim, H. Jeon, K.-I. Jang, Y.-W. Kim, C.-H. Im, and S.-H. Lee, "Mismatch negativity and cortical thickness in patients with schizophrenia and bipolar disorder," *Schizophrenia Bull.*, vol. 45, no. 2, pp. 425–435, Mar. 2019.
- [71] T. Miyanishi, T. Sumiyoshi, Y. Higuchi, T. Seo, and M. Suzuki, "LORETA current source density for duration mismatch negativity and neuropsychological assessment in early schizophrenia," *PLoS ONE*, vol. 8, no. 4, Apr. 2013, Art. no. e61152.
- [72] P. G. Nestor *et al.*, "Dissociable contributions of MRI volume reductions of superior temporal and fusiform gyri to symptoms and neuropsychology in schizophrenia," *Schizophrenia Res.*, vol. 91, nos. 1–3, pp. 103–106, Mar. 2007.
- [73] W. R. Fulham *et al.*, "Mismatch negativity in recent-onset and chronic schizophrenia: A current source density analysis," *PLoS ONE*, vol. 9, no. 6, Jun. 2014, Art. no. e100221.
- [74] C. C. Schultz *et al.*, "Increased parahippocampal and lingual gyration in first-episode schizophrenia," *Schizophrenia Res.*, vol. 123, nos. 2–3, pp. 137–144, Nov. 2010.
- [75] E. Başar and G. Dumermuth, "EEG-brain dynamics: Relation between EEG and brain evoked potentials," *Comput. Programs Biomed.*, vol. 14, no. 2, pp. 227–228, Apr. 1982.
- [76] L. E. Hong, L. V. Moran, X. Du, P. O'Donnell, and A. Summerfelt, "Mismatch negativity and low frequency oscillations in schizophrenia families," *Clin. Neurophysiol.*, vol. 123, no. 10, pp. 1980–1988, Oct. 2012.